Acta Crystallographica Section F
Structural Biology and Crystallization Communications
ISSN 1744-3091

Structure of the signal transduction protein TRAP (target of RNAIII-activating protein)

Kim Henrick[a] and Miriam Hirshberg[b]*‡

[a]Research Collaboratory for Structural Bioinformatics Protein Data Bank (RCSB PDB), Department of Chemistry and Chemical Biology, Rutgers, The State University of New Jersey, 610 Taylor Road, Piscataway, NJ 08854-8087, USA, and [b]Department of Biochemistry, University of Cambridge, 80 Tennis Court Road, Cambridge CB2 1GA, England

‡ Present address: Protein Data Bank in Europe, EMBL–EBI, Wellcome Trust Genome Campus, Hinxton, Cambridge CB10 1SD, England.

Correspondence e-mail: miri@ebi.ac.uk

Received 19 March 2012
Accepted 4 May 2012

PDB Reference: TRAP, 4ae5.

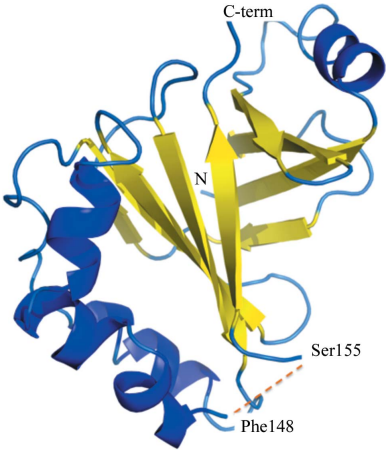

The crystal structure of the signal transduction protein TRAP is reported at 1.85 Å resolution. The structure of TRAP consists of a central eight-stranded β-barrel flanked asymmetrically by helices and is monomeric both in solution and in the crystal structure. A formate ion was found bound to TRAP identically in all four molecules in the asymmetric unit.

1. Introduction

Staphylococcus aureus is a Gram-positive bacterium that is part of the normal healthy flora of skin but that can become virulent and cause infections by producing biofilms and toxins. The production of virulence factors is regulated by cell–cell communication (quorum sensing) through histidine phosphorylation of target of RNAIII-activating protein (TRAP) and through the activation of the *agr* gene locus (Novick & Geisinger, 2008). TRAP is a membrane-associated 167-amino-acid protein with no transmembrane domain which is highly conserved among staphylococci (Balaban *et al.*, 2001; Gov *et al.*, 2004; Leitner *et al.*, 2011). TRAP phosphorylation, which can be induced by the autoinducer RNAIII-activating protein (RAP), was originally thought to lead to activation of the *agr* quorum-sensing system, resulting in the production of a regulatory mRNA molecule termed RNAIII and leading to toxin production and pathogenesis (Balaban *et al.*, 2001). A recent study by Kiran & Balaban (2009) demonstrated that TRAP does not regulate the *agr* system but rather protects DNA from oxidative damage and from spontaneous and adaptive (*agr*) mutations. Protein–protein interaction studies using a bacterial two-hybrid system have identified OpuCA as a TRAP-binding protein (Kiran *et al.*, 2009). OpuCA is an ATP-binding cytoplasmic (ABC) domain of the OpuC ABC transporter. TRAP has also been investigated in vaccine development for preventing staphylococcal mastitis in dairy cows (Leitner *et al.*, 2011). TRAP is conserved among all strains and species and is constitutively expressed in all strains of *S. aureus* or coagulase-negative staphylococcus tested to date, including those isolated from cows. TRAP may thus serve as a universal anti-staphylococcus vaccine. TRAP has high structural homology to YhgC in bacilli (Kiran *et al.*, 2010). Like TRAP in *S. aureus*, YhgC has been shown to be involved in stress response in *Bacillus anthracis* (Kiran *et al.*, 2010). However, the precise function and protein chemistry of TRAP is not fully understood.

2. Materials and methods

2.1. Protein expression, purification and crystallization

The recombinant TRAP protein was cloned and expressed in *Escherichia coli* as described previously (Kiran & Balaban, 2009) and was prepared by C&P Biotech Corporation, Canada. The hanging-drop vapour-diffusion method was used for crystallization, with the crystallization well containing 18% PEG 4K, 0.05 *M* sodium citrate pH 5.66, 1% PEG 500 MME and the drop consisting of a 1:1 volume ratio of protein solution (4.4 mg ml^{-1} in 50 m*M* Tris pH 8.0, 150 m*M*

NaCl, 1 m*M* DTT) and crystallization solution. Crystals formed within several days and were subsequently cryoprotected using 20% PEG 4K, 0.05 *M* sodium citrate, 1% PEG 500 MME, 35% PEG 400, which was followed by flash-cooling directly in liquid nitrogen. For SAD phasing, a potassium iodide soak was carried out using the method of Dauter *et al.* (2000). [Note: Han *et al.* (2005) reported the crystallization of TRAP from *S. aureus* in space group $P2_12_12_1$ using PEG 8000 and 5% Jeffamine M600 pH 7.0, but no subsequent structure was published.]

2.2. Data collection and structure determination

Diffraction data for native and KI-soaked TRAP were collected using an ADSC CCD detector on SRS beamline PX14.1 at a wavelength of 1.2445 Å and with an in-house R-AXIS IV (Biochemistry Department, University of Cambridge, England) at a wavelength of 1.5418 Å, respectively. Each of the two data sets were measured from a single crystal maintained at 100 K and the reflections were indexed, integrated and scaled using *HKL*-2000 (Otwinowski & Minor, 1997). The space group of the complex was $P2_1$, with four molecules in the asymmetric unit. Initial attempts to solve the structure by molecular-replacement methods with *Phaser* (McCoy *et al.*, 2007) using models built by either *MODBASE* (Pieper *et al.*, 2011) or *SWISS-MODEL* (Arnold *et al.*, 2006) failed to give a clear solution. Direct molecular replacement with *BALBES* (Long *et al.*, 2008) also failed. These

Table 1
Crystallographic data and refinement information.

Values in parentheses are for the highest resolution shell.

	TRAP, native	TRAP, KI soak
Space group	$P2_1$	$P2_1$
Unit-cell parameters (Å, °)	a = 69.076, b = 70.868, c = 79.082, β = 111.53	a = 69.021, b = 71.217, c = 79.020, β = 110.793
Resolution range (Å)	74.5–1.85 (1.90–1.85)	32.8–2.35 (2.48–2.35)
Total observations	705734	462053
Unique reflections	60732	29545
Completeness (%)	92.1 (79.5)	98.7 (98.5)
Multiplicity	3.5 (3.1)	7.0 (7.0)
$\langle I/\sigma(I)\rangle$	21.9	21.7
$R_{\rm merge}$†	0.04 (0.23)	0.07 (0.28)
$R_{\rm cryst}/R_{\rm free}$‡	0.211 (0.259)	0.23 (0.29)
Protein atoms	5404	5442
Heterogen atoms	12	29
Solvent molecules	262	56
Average B factor (Å^2)	19.03	36.13
R.m.s.d. bond lengths (Å)	0.019	0.020
R.m.s.d. bond angles (°)	1.925	1.926
Ramachandran plot§ (%)		
Most favoured	93.3	91.3
Additionally allowed	6.7	6.9
Generously allowed	0	1.8
Disallowed	0	0

† $R_{\rm merge} = \sum_{hkl}\sum_i |I_i(hkl) - \langle I(hkl)\rangle|/\sum_{hkl}\sum_i I_i(hkl)$, where $I(hkl)$ is the intensity of reflection hkl. ‡ $R_{\rm cryst}$ and $R_{\rm free} = \sum_{hkl}\big||F_{\rm obs}| - |F_{\rm calc}|\big|/\sum_{hkl}|F_{\rm obs}|$, where $F_{\rm obs}$ and $F_{\rm calc}$ are the observed and calculated amplitudes, respectively. $R_{\rm free}$ was calculated using 5% of data excluded from model building and refinement. § Laskowski *et al.* (1993).

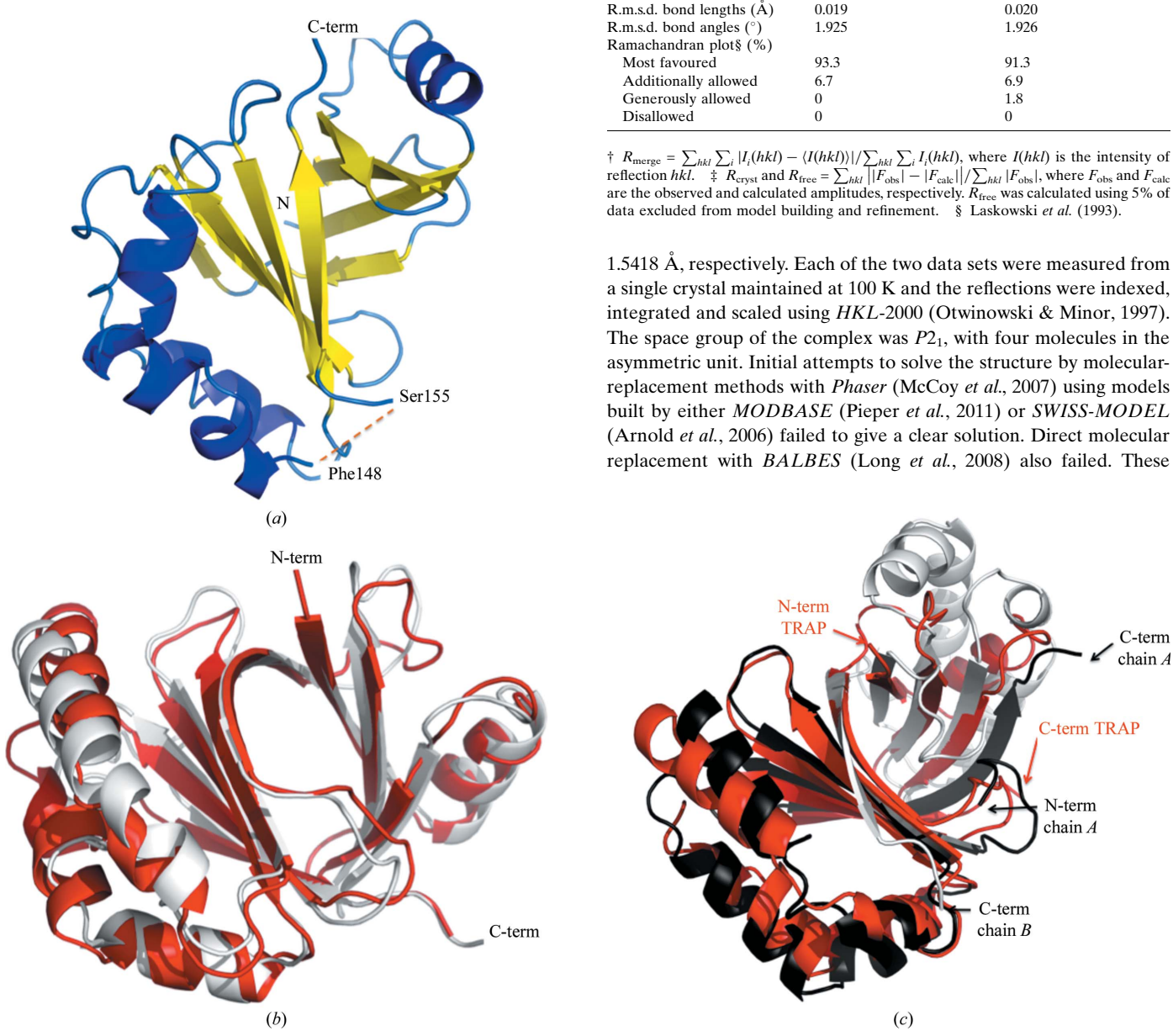

Figure 1
(*a*) The overall structure of TRAP. (*b*) A superposition of TRAP (in red) with the model obtained using *SWISS-MODEL* based on PDB entry 3fez (white); the r.m.s.d. is 1.85 Å over 136 Cα atoms. All figures were produced using *PyMOL* (Schrödinger LLC) and all superpositions were carried out with *SSM* (Krissinel & Henrick, 2004). (*c*) Superposition of TRAP (red) with the homodimeric monooxygenase ACTVA-ORF6 from *S. coelicolor* (PDB enry 1n5v); the two identical chains are shown in white and black and the r.m.s.d. is 2.36 Å over 139 Cα atoms.

methods all used models based on a combination of an uncharacterized ferredoxin-fold protein related to antibiotic biosynthesis monooxygenases and a monoxygenase-like protein (PDB codes 3fez and 3fj2, respectively; Joint Center for Structural Genomics, unpublished work). The initial phases were determined by the SAD method using *PHENIX* (Adams *et al.*, 2010; Terwilliger *et al.*, 2009) with the potassium iodide derivative. Initial phases were calculated from 28 iodine sites with a score of 0.421 (3–15 Å resolution, 9997 reflections, σ cutoff 0.5), followed by automatic NCS detection, resulting in an overall figure of merit of 0.69 and an average correlation coefficient of 0.74. Starting from the SAD-phased map, *ARP*/*wARP* (Cohen *et al.*, 2008) automatically built more than 160 residues of each of the four copies in the asymmetric unit.

The structure was determined by iterative rounds of positional refinement using *REFMAC*5 (Murshudov *et al.*, 2011) with the model-building software suite *Coot* (Emsley *et al.*, 2010). Individual *B* factors were refined using an overall anisotropic *B*-factor refinement together with bulk-solvent correction. The solvent and formate ions were built into the density in later rounds of refinement. Data for TRAP–KI were used for an incomplete refinement, which gave 29 iodine sites. Data-collection and refinement statistics are shown in Table 1.

3. Results and discussion

3.1. Overall structure of TRAP

TRAP is a monomer both in the crystal structure and in solution (data from SAXS studies; not shown). The overall fold of TRAP is a central eight-stranded β-barrel surrounded by one α-helix on one side and four α-helices on the opposite side (Fig. 1*a*). The fold is very similar to the fold of the models that were used in our unsuccessful molecular-replacement attempts. Fig. 1(*b*) shows a superposition of the model from *SWISS-MODEL* used in the molecular-replacement trials and TRAP. The TRAP protein has a similar overall fold to dimeric monooxygenase enzymes such as that encoded by the ACTVA-ORF6 gene of *Streptomyces coelicolor* (PDB entry 1n5v; Sciara *et al.*, 2003); however, TRAP adopts a nonsymmetrical arrangement of the helices (Fig. 1*c*).

3.2. Formate ion

A bent three-atom molecule is clearly visible in the density map, occupying an identical site in all four copies in the asymmetric unit (Fig. 2*a*). It is hydrogen bonded to two positively charged side chains (Lys115 and Arg 160) and is further stabilized by van der Waals interactions between its central atom and the side chain of Ala70 (Fig. 2*b*). This molecule could only be a negatively charged ion, either nitrite or formate. Both formate and nitrite are known to be involved in *S. aureus* gene expression (Fuchs *et al.*, 2007). The same site is occupied by an iodine ion in the potassium iodide soak structure (data not shown). We have chosen to represent this density as a formate ion, as this is more likely to have been bound to the protein during expression in *E. coli* or in subsequent purification steps (carried out by C&P Biotech Corp.). The TRAP formate-binding site consists of Thr6, Tyr8, Ala70, Phe72, Lys115, Tyr117 and Arg160, all of which are 100% conserved within conserved groups of residues

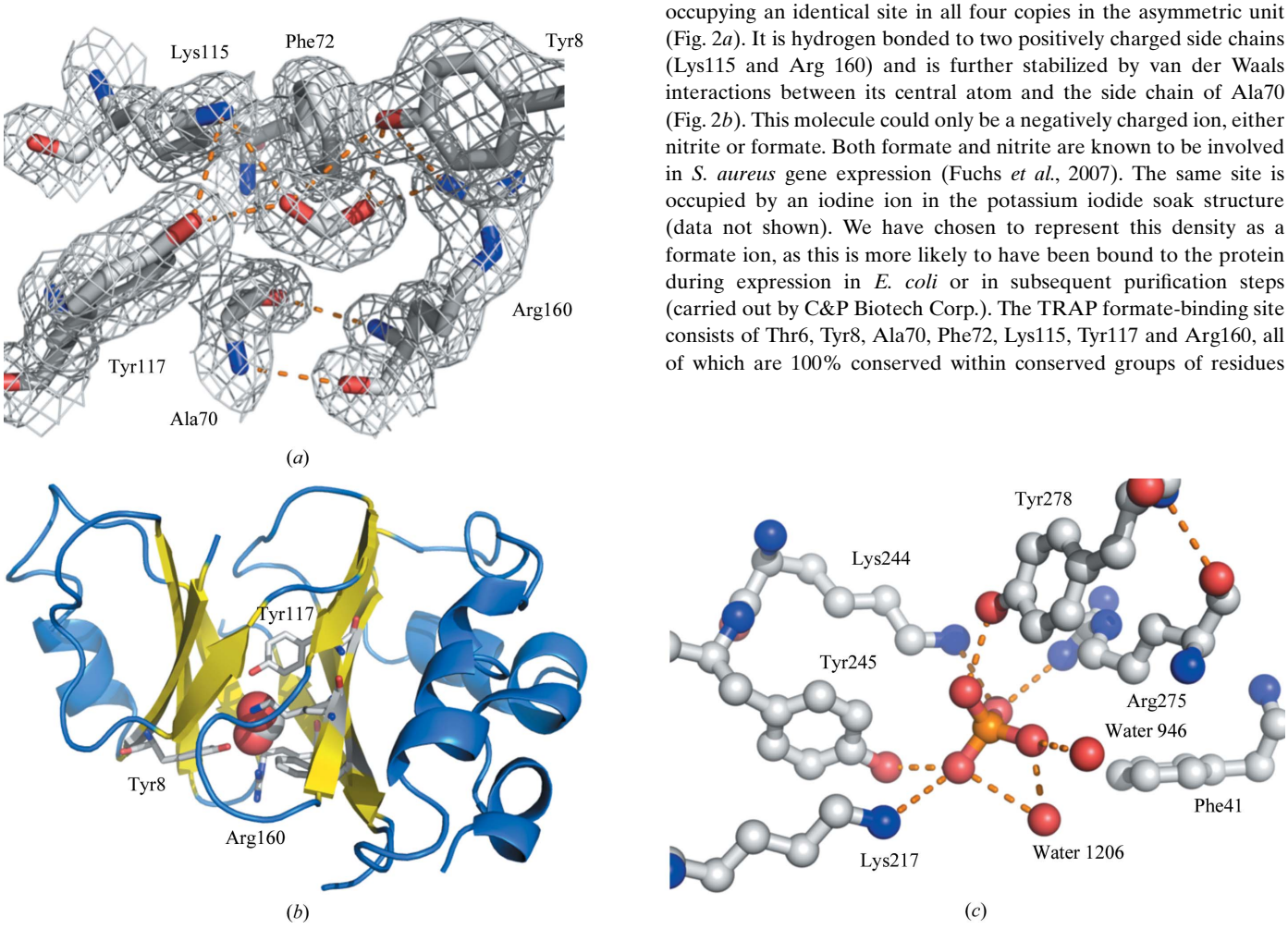

Figure 2
(*a*, *b*) The formate ion-binding site of TRAP. The site consists of hydrogen-bonding side chains from Tyr8, Lys115, Tyr117 and Arg160, with van der Waals contacts with Phe72 and Ala70. The main-chain atoms of Ala70 hold the Arg160 side chain in place. (*a*) $3F_o - 2F_c$ electron-density map at the 1.0σ level of the binding site. (*b*) The location of the site in the overall TRAP fold. The formate is shown as a stick model in (*a*) and as a CPK model in (*b*); hydrogen bonds are indicated by dotted orange lines. (*c*) The phosphate-binding site of amidohydrolase from *M. synoviae* (PDB entry 3ovg; New York SGX Research Center for Structural Genomics, unpublished work). Colour scheme: phosphate ion, orange; amino-acid C atoms, grey; amino-acid O atoms, red; amino-acid N atoms, blue. Water molecules are shown as red spheres and hydrogen bonds as orange broken lines.

along the peptide in an alignment of 17 TRAP sequences across *Staphylococcus* strains (Fig. 4*b*).

A phosphate-binding site similar to the formate site in TRAP was identified using *PDBeSITE* (Golovin & Henrick, 2008; Golovin *et al.*, 2005) in an amidohydrolase from *Mycoplasma synoviae* with a Zn ion bound independent of the phosphate site (PDB entry 3ovg; New York SGX Research Center for Structural Genomics, unpublished work). The phosphate-binding site consists of Lys217, Lys244, Tyr24, Arg275, Tyr278 and Phe41 and is shown in Fig. 2(*c*). The buried nature of the formate found in TRAP and the methyl group of the nearby Ala70 residue suggests that although the two sites have some similarity, the site in TRAP may not accommodate a phosphate ion.

3.3. Possible haem- and divalent metal-binding sites

The two dimeric haem-degrading enzymes in *S. aureus*, IsdG and IsdI (PDB entries 2zdo and 2zdp, respectively; Lee *et al.*, 2008), have almost the same fold as TRAP (Fig. 3*a*). The *3DLigandSite* software (Wass *et al.*, 2010) suggests that TRAP could bind a haem molecule but only on one side of the β-barrel, whereas other closely related haem-binding proteins are homodimeric and symmetrical (see, for example, Gaballa & Helmann, 2011). It is thus most likely that TRAP is derived from an original haem oxygenase fold but has evolved to have a different function.

Based on the structure of the hypothetical protein TT1380 from *Thermus thermophilus* (PDB entry 1iuj; Wada *et al.*, 2004), *3DLigandSite* predicted a zinc-binding site in TRAP around residues Tyr157 and Glu159. The hypothetical protein TT1380 is a symmetrical homodimer with a fold similar to TRAP. The environment of Tyr157 and Glu159 is the same in all four copies of TRAP in the asymmetric unit, with the site in chain *A* shown in Fig. 3(*b*). The three water molecules 2016, 2019 and 2064 have *B* factors of 36.7, 37.0 and 32.7 Å^2, respectively. Fig. 3(*c*) shows a superposition of TRAP with PDB entry 1iuj; however, it is uncommon for a zinc-binding site to lack a histidine residue, as is suggested by *3DLigandSite* for the zinc-binding site of TRAP.

3.4. His residues

TRAP is highly conserved in staphylococci and contains three conserved histidine residues (His66, His79 and His154) across 17 *S. aureus* strains (see Fig. 1 of Gov *et al.*, 2004 and Fig. 4*b*). These histidine residues have been suggested to be phosphorylated (Gov *et al.*, 2004), but their importance in pathogenesis has yet to be determined (Shaw *et al.*, 2007). As shown here, TRAP, with its eight strands and five helices, is an incomplete $(\beta/\alpha)_8$-barrel structure, although the related symmetrical dimers (see above) such as in PDB entry 1n5v are closer to a $(\beta/\alpha)_8$-barrel, having eight helices and ten strands. By analogy with the observation that the active sites of all $(\beta/\alpha)_8$-barrels are located on the C-terminal face of the central β-barrel (Vega *et al.*, 2003; Nagano *et al.*, 2002; Wierenga, 2001), His66, together with an additional less conserved His65, are positioned on the C-terminal

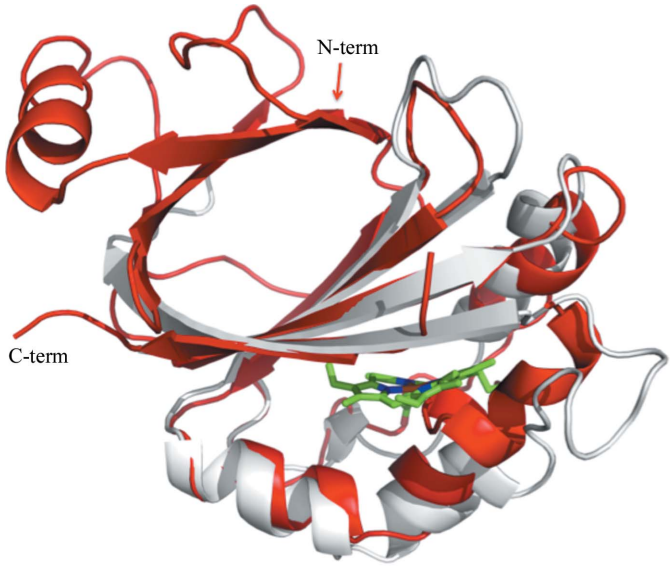

(*a*)

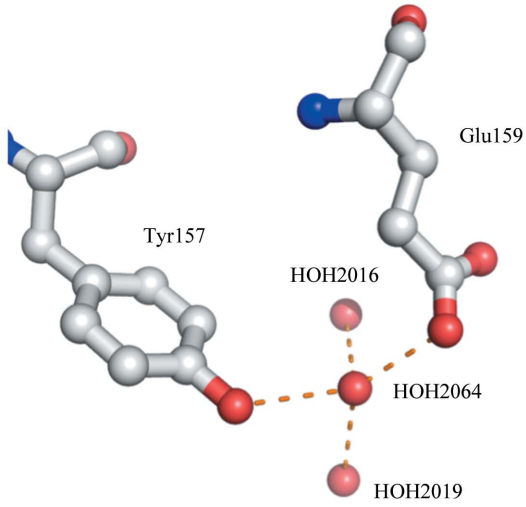

(*b*)

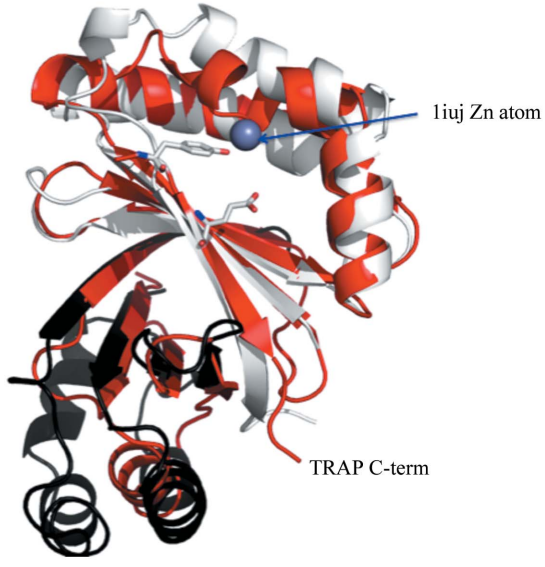

(*c*)

Figure 3
Predicted ligand-binding sites. (*a*) Superposition of TRAP (red) with a single chain of the *S. aureus* dimeric haem-degrading enzyme IsdG (PDB entry 2zdo; white; r.m.s.d. of 1.87 Å over 81 C$^\alpha$ atoms). The 2zdo haem group is shown as a stick model. (*b*) A predicted zinc-binding site in TRAP. Water molecules occupying the site in the present crystal structure are shown as red balls, hydrogen bonds are shown as broken orange lines and amino acids are shown as ball-and-stick models. (c) Superposition of TRAP (red) with the homodimeric structure 1iuj (black and white chains; r.m.s.d. of 2.04 Å over 136 C$^\alpha$ atoms) indicating TRAP residues Tyr157 and Glu159 and the position of the zinc ion in TT1380.

face of the TRAP β-barrel (Fig. 4*a*) and are likely to have an important role. His66 may be especially significant as residues 66–68 (HFY) are completely conserved (Fig. 4*b*). His79 and His154 are located on the opposite side of the TRAP barrel and thus are unlikely to have a key role. His154 is in a completely conserved block of residues (153–164; QHSSYFERYLYP), while His79 is a single isolated point of conservation (Fig. 4*b*).

3.5. Quaternary structures and the disordered loop

Residues 149–154 (sequence Gly-Ser-Ser-Gly-Gln-His) are unobserved in each of the four copies of TRAP in the crystal structure. Attempts to generate a plausible loop for these residues with the *Robetta* server (Raman *et al.*, 2009) did not give a model in which the loop was free of crystal contacts. The *Phyre* server (Kelley & Sternberg, 2009), using the 'one-to-one threading' option, did give a possible loop structure and a *REFMAC*5 refinement run gave a structure without crystal contacts and acceptable geometry. Unfortunately, the density correlation was very poor.

PDB entry 1iuj used above to predict a plausible zinc-binding site in TRAP has a tetramer generated by *PISA* (Krissinel & Henrick, 2007) recorded in the PDB entry, with a buried surface area of 8650 Å^2 (Fig. 5*a*). This tetramer has its two barrels side by side with their axes approximately parallel. A deep cleft is produced upon formation of the dimer of dimers, with the walls of the cleft consisting of residues 7–10 and 87–93 and the floor made up of residues 46–49 from all four chains. Structural alignment of two molecules of TRAP with the 1iuj tetramer without any attempt at optimization yielded a looser packed dimer in which the cleft is made up of residues 72–75, 156–162 and 32–35, which correspond to the residue ranges listed above in PDB entry 1iuj (Fig. 5*b*). Contained within these residues are two key residues for formate binding, namely Arg160 and Phe72 (see above). We speculate that for TRAP dimer formation the formate has to disassociate from the protein, allowing Arg160 to form a strong salt bridge across the dimer interface with Asp33. Asp33 is 100% conserved within the 32–35 region of conserved sequence [D(S/T)S]. Our analysis suggests that by analogy the TRAP regions discussed here could be part of a 'sticky patch' (Philo & Arakawa, 2009) that might be involved in either homodimer or heterocomplex formation. In addition, the disordered loop located close to this dimer interface could adopt an ordered conformation upon binding to a second protein in which the conserved His154 might have a role.

3.6. Sequence/function/fold

The TRAP sequence contains an antibiotic biosynthesis monooxygenase (ABM) domain (Sciara *et al.*, 2003; residues 77–139). The ABM domain is described in Pfam (Punta *et al.*, 2012) as having only moderate sequence homology while sharing a high degree of structural similarity. KEGG (Kanehisa *et al.*, 2012) lists proteins that contain an ABM domain that are involved in a diverse range of biological processes, including metabolism, transcription, translation and biosynthesis of secondary metabolites. *B. anthracis* YhgC, which is a homologue of TRAP (Kiran *et al.*, 2010), also contains an ABM

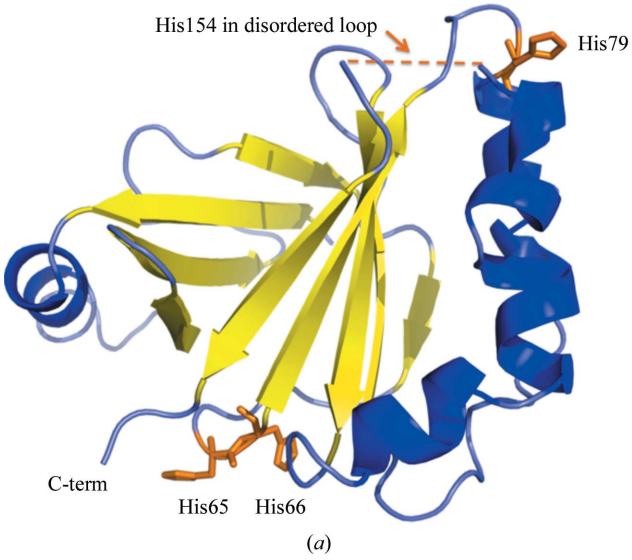

(*a*)

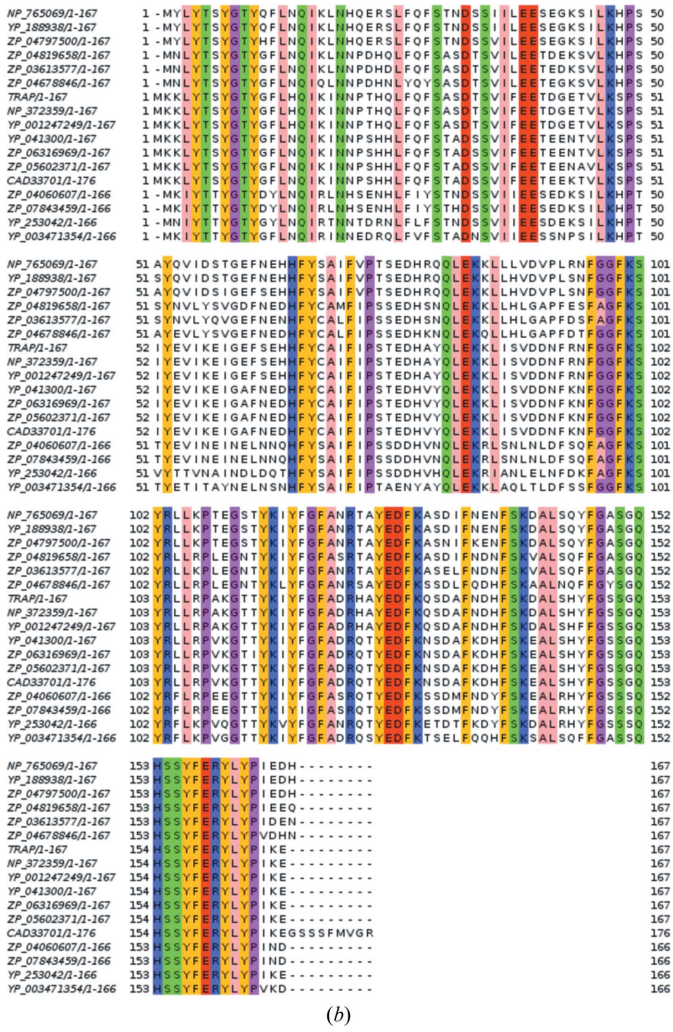

(*b*)

Figure 4
Histidines in TRAP. (*a*) Histidines 65, 66 and 79 are denoted as orange stick models. Note that His154 is unobserved in the present crystal structure. His79 and His154 are located near the disordered loop 149–154, while His65 and His66 are positioned on the C-terminal face of the TRAP β-barrel. (*b*) *JalView* (Waterhouse *et al.*, 2009) alignment of TRAP with other *Staphylococcus* strains. The alignment is coloured at 75% identity using the Zappo colouring scheme. The strains of the sequences presented are TRAP (*S. aureus* RN6390B ATCC 55620), CAD33701 (*S. aureus*), NP_372359 (*S. aureus* subsp. *aureus* Mu50), YP_041300 (*S. aureus* subsp. *aureus* MRSA2520), ZP_06316969 (*S. aureus* subsp. *aureus* WW2703/97), ZP_05602371 (*S. aureus* subsp. *aureus* 55/2053), YP_001247249 (*S. aureus* subsp. *aureus* JH9), YP_003471354 (*S. lugdunensis* HKU09-01), NP_765069 (*S. epidermidis* ATCC 12228), YP_188938 (*S. epidermidis* RP62A), ZP_04797500 (*S. epidermidis* W23144), ZP_04819658 (*S. epidermidis* M23864:W1), ZP_03613577 (*S. capitis* SK14), ZP_04678846 (*S. warneri* L37603), ZP_04060607 (*S. hominis* SK119), ZP_07843459 (*S. hominis* subsp. *hominis* C80) and YP_253042 (*S. haemolyticus* JCSC1435).

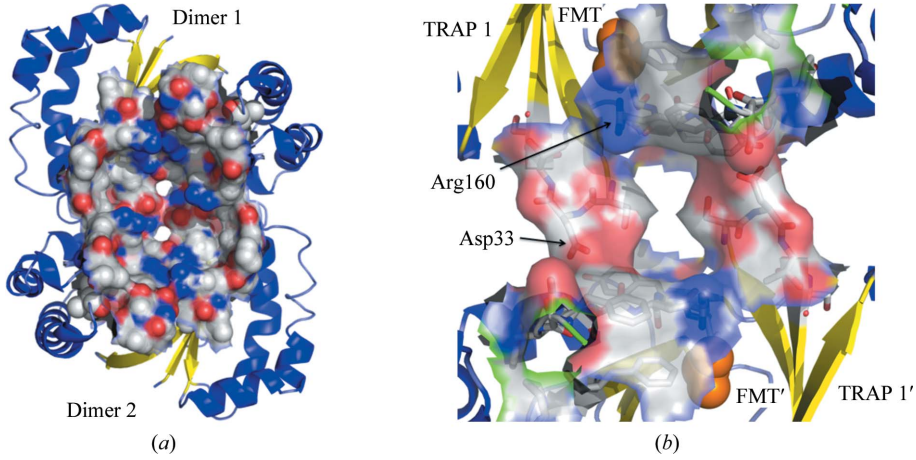

Figure 5
Potential TRAP dimer. (*a*) The structure of the 1iuj dimer of dimers as recorded in its PDB entry, showing the cleft formed at the dimer–dimer interface and represented as a surface. (*b*) TRAP molecules superposed on the 1iuj dimer of dimers, showing the formate as van der Waals spheres (orange) and the surface of the TRAP residues that correspond to the 1iuj interface residues; the residues that flank the unobserved loop, 148 and 155, are shown in green. Arg160 and Asp33 are discussed in the text.

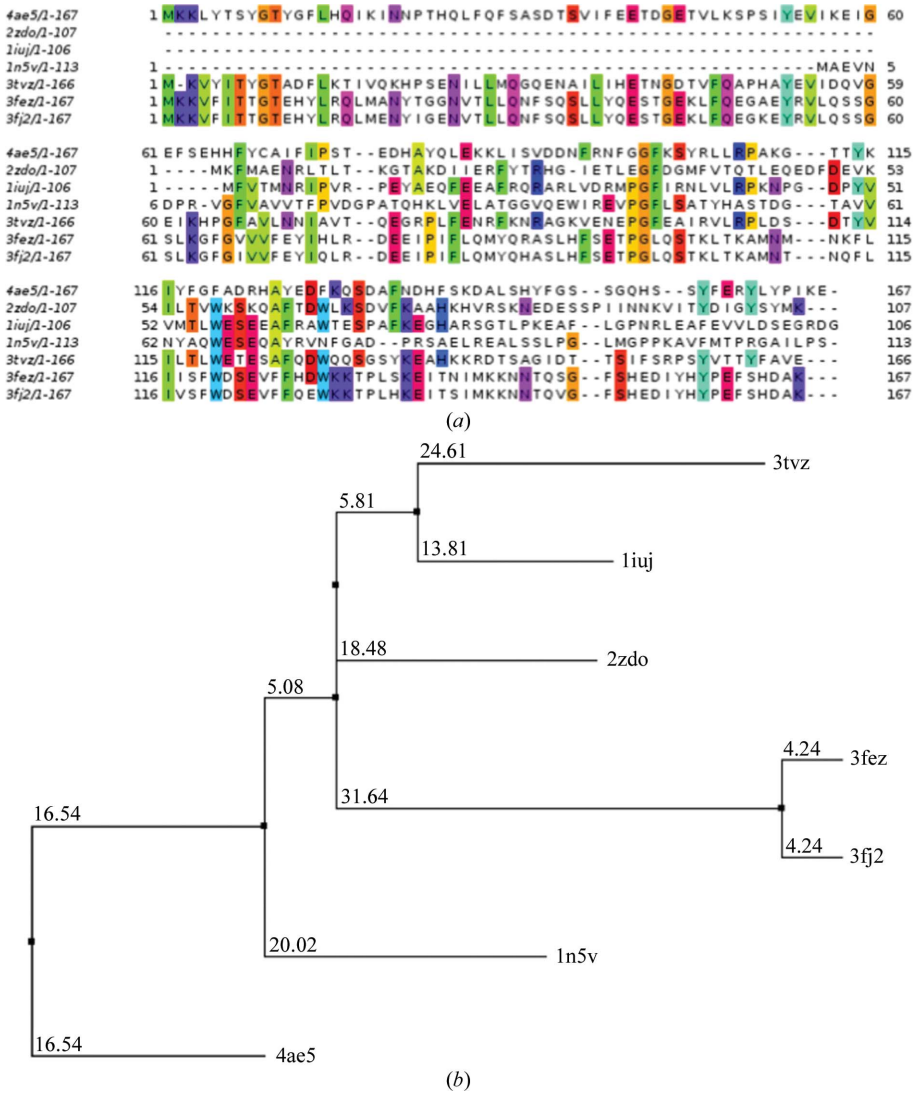

Figure 6
(*a*) *JalView* alignment of the TRAP-related proteins mentioned in this paper. It is apparent that although the structures discussed here have a close structural homology to TRAP, there is little sequence homology. Species: 4ae5 and 2zdo, *Staphylococcus aureus*; 1iuj, *Thermus thermophilus*; 1n5v, *Streptomyces coelicolor*; 3fez, *Listeria monocytogenes*; 3fj2, *L. innocua*; 3tvz, *Bacillus subtilis*. (*b*) A *JalView*-generated dendrogram created using the neighbour-joining algorithm option also suggests that TRAP is potentially close to an unknown parent gene rather any other sequence given here.

domain. This protein is also present in *B. subtilis* as a member of the IsdG family of haem oxygenases designated HmoB (formally YhgC; Gaballa & Helmann, 2011). A structure for the latter has been deposited in the PDB (PDB entry 3tvz; J. Choe, S. Choi & S. Park, unpublished work). In our view, the ABM domain is unlikely to have any real significance in TRAP. There is little sequence alignment for the structures discussed in this paper (Fig. 6) and it is unlikely that TRAP shares any of their functionality.

4. Conclusion

The crystal structure of TRAP from *S. aureus* solved by SAD and refined to 1.85 Å resolution reveals an asymmetric eight-stranded five-helix barrel. Structural and sequence analysis revealed an unexpected binding site occupied in the crystal structure by a formate ion and points to the probable importance of Arg160, His66 and the disordered loop in protein–protein interaction with a binding partner. Additional structural and biological research is needed to decipher the structure–function relationship of TRAP.

The initial work of crystallization and data collection was carried out while MH was a research associate in the laboratory of Professor E. D. Laue in the Biochemistry Department at the University of Cambridge, England.

References

Adams, P. D. *et al.* (2010). *Acta Cryst.* D**66**, 213–221.
Arnold, K., Bordoli, L., Kopp, J. & Schwede, T. (2006). *Bioinformatics*, **22**, 195–201.
Balaban, N., Goldkorn, T., Gov, Y., Hirshberg, M., Koyfman, N., Matthews, H. R., Nhan, R. T., Singh, B. & Uziel, O. (2001). *J. Biol. Chem.* **276**, 2658–2667.
Cohen, S. X., Ben Jelloul, M., Long, F., Vagin, A., Knipscheer, P., Lebbink, J., Sixma, T. K., Lamzin, V. S., Murshudov, G. N. & Perrakis, A. (2008). *Acta Cryst.* D**64**, 49–60.
Dauter, Z., Dauter, M. & Rajashankar, K. R. (2000). *Acta Cryst.* D**56**, 232–237.
Emsley, P., Lohkamp, B., Scott, W. G. & Cowtan, K. (2010). *Acta Cryst.* D**66**, 486–501.
Fuchs, S., Pané-Farré, J., Kohler, C., Hecker, M. & Engelmann, S. (2007). *J. Bacteriol.* **189**, 4275–4289.
Gaballa, A. & Helmann, J. D. (2011). *Microbiology*, **157**, 3221–3231.
Golovin, A., Dimitropoulos, D., Oldfield, T., Rachedi, A. & Henrick, K. (2005). *Proteins*, **58**, 190–199.
Golovin, A. & Henrick, K. (2008). *BMC Bioinformatics*, **9**, 312.
Gov, Y., Borovok, I., Korem, M., Singh, V. K., Jayaswal, R. K., Wilkinson, B. J., Rich, S. M. & Balaban, N. (2004). *J. Biol. Chem.* **279**, 14665–14672.
Han, Y.-H., Kim, Y.-G., Kim, D. Y., Ha, S. C., Lokanath, N. K. & Kim, K. K. (2005). *Biochim. Biophys. Acta*, **1748**, 134–136.
Kanehisa, M., Goto, S., Sato, Y., Furumichi, M. & Tanabe, M. (2012). *Nucleic Acids Res.* **40**, D109–D114.
Kelley, L. A. & Sternberg, M. J. (2009). *Nature Protoc.* **4**, 363–371.
Kiran, M. D., Akiyoshi, D. E., Giacometti, A., Cirioni, O., Scalise, G. & Balaban, N. (2009). *Int. J. Artif. Organs*, **32**, 600–610.
Kiran, M. D., Bala, S., Hirshberg, M. & Balaban, N. (2010). *Int. J. Artif. Organs*, **33**, 590–607.
Kiran, M. D. & Balaban, N. (2009). *Int. J. Artif. Organs*, **32**, 592–599.
Krissinel, E. & Henrick, K. (2004). *Acta Cryst.* D**60**, 2256–2268.
Krissinel, E. & Henrick, K. (2007). *J. Mol. Biol.* **372**, 774–797.
Laskowski, R. A., MacArthur, M. W., Moss, D. S. & Thornton, J. M. (1993). *J. Appl. Cryst.* **26**, 283–291.
Lee, W. C., Reniere, M. L., Skaar, E. P. & Murphy, M. E. P. (2008). *J. Biol. Chem.* **283**, 30957–30963.
Leitner, G., Krifucks, O., Kiran, M. D. & Balaban, N. (2011). *Vet. Immunol. Immunopathol.* **142**, 25–35.
Long, F., Vagin, A. A., Young, P. & Murshudov, G. N. (2008). *Acta Cryst.* D**64**, 125–132.
McCoy, A. J., Grosse-Kunstleve, R. W., Adams, P. D., Winn, M. D., Storoni, L. C. & Read, R. J. (2007). *J. Appl. Cryst.* **40**, 658–674.
Murshudov, G. N., Skubák, P., Lebedev, A. A., Pannu, N. S., Steiner, R. A., Nicholls, R. A., Winn, M. D., Long, F. & Vagin, A. A. (2011). *Acta Cryst.* D**67**, 355–367.
Nagano, N., Orengo, C. A. & Thornton, J. M. (2002). *J. Mol. Biol.* **321**, 741–765.
Novick, R. P. & Geisinger, E. (2008). *Annu. Rev. Genet.* **42**, 541–564.
Otwinowski, Z. & Minor, W. (1997). *Methods Enzymol.* **276**, 307–326.
Philo, J. S. & Arakawa, T. (2009). *Curr. Pharm. Biotechnol.* **10**, 348–351.
Pieper, U. *et al.* (2011). *Nucleic Acids Res.* **39**, 465–474.
Punta, M. *et al.* (2012). *Nucleic Acids Res.* **40**, D290–D301.
Raman, S. *et al.* (2009). *Proteins*, **77**, Suppl. 9, 89–99.
Sciara, G., Kendrew, S. G., Miele, A. E., Marsh, N. G., Federici, L., Malatesta, F., Schimperna, G., Savino, C. & Vallone, B. (2003). *EMBO J.* **22**, 205–215.
Shaw, L. N., Jonsson, I.-M., Singh, V. K., Tarkowski, A. & Stewart, G. C. (2007). *Infect. Immun.* **75**, 4519–4527.
Terwilliger, T. C., Adams, P. D., Read, R. J., McCoy, A. J., Moriarty, N. W., Grosse-Kunstleve, R. W., Afonine, P. V., Zwart, P. H. & Hung, L.-W. (2009). *Acta Cryst.* D**65**, 582–601.
Vega, M. C., Lorentzen, E., Linden, A. & Wilmanns, M. (2003). *Curr. Opin. Chem. Biol.* **7**, 694–701.
Wada, T., Shirouzu, M., Terada, T., Kamewari, Y., Park, S.-Y., Tame, J. R. H., Kuramitsu, S. & Yokoyama, S. (2004). *Proteins*, **55**, 778–780.
Wass, M. N., Kelley, L. A. & Sternberg, M. J. (2010). *Nucleic Acids Res.* **38**, W469–W473.
Waterhouse, A. M., Procter, J. B., Martin, D. M., Clamp, M. & Barton, G. J. (2009). *Bioinformatics*, **25**, 1189–1191.
Wierenga, R. K. (2001). *FEBS Lett.* **492**, 193–198.